研究成果の刊行物・別刷り

（分担者）

Immunogenetics (2012) 64:15–29
DOI 10.1007/s00251-011-0556-2

ORIGINAL PAPER

Positive selection of Toll-like receptor 2 polymorphisms in two closely related old world monkey species, rhesus and Japanese macaques

Akiko Takaki · Akiko Yamazaki · Tomoyuki Maekawa · Hiroki Shibata · Kenji Hirayama · Akinori Kimura · Hirohisa Hirai · Michio Yasunami

Received: 7 January 2011 / Accepted: 21 June 2011 / Published online: 9 July 2011

Abstract Toll-like receptor 2 (TLR2) plays an important role in the recognition of a variety of pathogenic microbes. In the present study, we compared polymorphisms of *TLR2* locus in two closely related old world monkey species, rhesus monkey (*Macaca mulatta*) and Japanese monkey (*Macaca fuscata*). By nucleotide sequencing of the third exon of *TLR2* gene from 21 to 35 respective individuals, we could assign 17 haplotype combinations of 17 coding SNPs of ten non-synonymous and seven synonymous substitutions. A non-synonymous substitution at codon position 326 appeared to be differentially fixed in each species, asparagine for *M. mulatta* whereas tyrosine for *M. fuscata*, and may contribute to certain functional properties because it locates in the region contributing to ligand binding and interaction with dimerization partner of TLR2-TLR1 heterodimeric complex. Although *TLR2* alleles have diverged to similar extent in both species, they have evolved in significantly different ways; *TLR2* of *M. fuscata* has undergone purifying selection while the membrane-proximal part of the extracellular domain of *M. mulatta TLR2* exhibits higher rates of non-synonymous substitutions, indicating a trace of Darwinian positive selection.

Keywords Innate immunity · TLR · Polymorphism · Nonhuman primate · Molecular evolution · Reporter gene assay

Electronic supplementary material The online version of this article (doi:10.1007/s00251-011-0556-2) contains supplementary material, which is available to authorized users.

A. Takaki · A. Yamazaki · H. Shibata · K. Hirayama · M. Yasunami (✉)
Department of Immunogenetics, Institute of Tropical Medicine, Nagasaki University,
1-12-4 Sakamoto,
Nagasaki 852-8523, Japan
e-mail: yasunami@nagasaki-u.ac.jp

A. Takaki · T. Maekawa · M. Yasunami
Department of Clinical Medicine, Institute of Tropical Medicine, Nagasaki University,
Nagasaki, Japan

A. Kimura
Department of Molecular Pathogenesis,
Medical Research Institute, Tokyo Medical and Dental University,
Tokyo, Japan

H. Hirai
Department of Cellular and Molecular Biology,
Primate Research Institute, Kyoto University,
Kyoto, Japan

Introduction

The rhesus macaque, *Macaca mulatta*, is one of the best known old world monkeys and has been used for various biomedical researches as a nonhuman primate model including infections of simian immunodeficiency virus (Ling et al. 2002; Matano et al. 2004) and *Mycobacterium tuberculosis* (McMurray 2000; Huang et al. 2007). *M. mulatta* belongs to the primate family Cercopithecidae that shares the last common ancestor of approximately 25 million years ago (Mya) with human and hominoids (Kumar and Hedges 1998). According to this fact, nucleotide sequence similarity between humans and *M. mulatta* has been maintained as high as 93% in average (Rhesus Macaque Genome Sequencing and Analysis Consortium 2007). Analyses of molecular evolution of mitochondrial and nuclear DNA among species of genus *Macaca* estimate the divergence between rhesus and

cynomolgus macaque, *Macaca fascicularis* at 0.9–2.5 Mya (Hayasaka et al. 1996; Blancher et al. 2008; Osada et al. 2008; Stevison and Kohn 2009). Japanese monkey, *Macaca fuscata* and Taiwanese monkey, *Macaca cyclopis* had been derived from the rhesus lineage relatively recently, and the geographical isolation is fundamental for the diversification of these species (Smith et al. 2007). *M. mulatta* has a relatively broad geographical distribution from Afghanistan across Asia to the Chinese shore of the Pacific Ocean (Rhesus Macaque Genome Sequencing and Analysis Consortium 2007), where the tropical infectious agents such as *Plasmodium* species and arthropod-borne viruses are circulating and may influence the host genome as selection pressure. To date, a number of comparative studies on primate genome including *Macaca* species have been conducted. Among them, immune-related genes such as *TNFA* (Baena et al. 2007), eosinophil cationic protein (*ECP*), and eosinophil-derived neurotoxin (*EDN*) ribonuclease (Zhang et al. 1998) are shown to be evolved under positive Darwinian selection (or diversifying selection), suggesting the presence of a differential pressure between primate species.

Toll-like receptors (TLRs) are the first line of the host defense mechanisms against pathogenic microorganisms as pattern-recognition receptors (PRRs) (Akira et al. 2006). A number of single nucleotide polymorphisms (SNPs) have been found in the components of the TLR signaling pathway in humans. Alterations of the structure of these signaling molecules are often associated with susceptibility to various infectious diseases. In the case of human TLR2 that binds to peptidoglycan and lipoteichoic acid derived from Gram-positive bacteria as well as a variety of macromolecules from other microbes (Texereau et al. 2005), a non-synonymous substitution of glutamine for arginine at amino acid position 753 (Arg753Gln) was shown to be a risk factor of developing tuberculosis (Bochud et al. 2003; Ogus et al. 2004) and septic shock (Lorenz et al. 2000), whereas, have a protective effect against the development of Lyme disease (Schröder et al. 2005). It is hypothesized that TLR2 is also variable in *Macaca* species and exhibits a trace of molecular evolution events which is conferred by possible differences in individual response to various infectious agents. Previous reports on molecular evolution of TLRs of primates, which support the functional conservation of intra-cellular signal transduction machinery involving a common functional cytoplasmic Toll/Interleukin-1 receptor (TIR) domain during mammalian evolution, also suggested the presence of the positive Darwinian selection on the extracellular domain of TLR4 in *Macaca* species (Sanghavi et al. 2004; Nakajima et al. 2008).

In the present study, SNPs in the coding sequence of TLR2 from two closely related *Macaca* species, *M. mulatta* and *M. fuscata* were investigated. By nucleotide sequencing of 21 *M. mulatta* and 35 *M. fuscata* individuals, ten non-synonymous and seven synonymous substitutions were identified in the coding region. These 17 SNPs compose 17 haplotype combinations (or alleles) existing in the examined population. The ratio of rates of non-synonymous versus synonymous substitutions suggested the conservation of overall amino acid sequence except for a part of extracellular domain of *M. mulatta* TLR2, where multiple amino acid substitutions have taken place to give rise different alleles. Although the functional difference of TLR2 alleles was not evident by in vitro transfection study of expression vector to HEK293 cells, molecular modeling suggested that modified receptor-ligand interaction conferred by amino acid substitution in *M. mulatta* TLR2 is a driving force of diversifying evolution.

Materials and methods

Genomic DNA samples

Individual genomic DNA of *M. mulatta* were prepared from B lymphoblastoid cell lines which had been established from peripheral blood of mutually unrelated founders of breeding colony originated from wild population in Myanmar and Laos as described before (Takahashi-Tanaka et al. 2007). Samples of peripheral blood of *M. fuscata* were collected from three isolated colonies originated from different wild populations in Japan maintained at Primate Research Institute, Kyoto University, after the institutional review of experimental procedures. Genomic DNA of leukocytes was isolated using Wizard® Genomic DNA Purification Kit (Promega).

Nucleotide sequencing of coding region of TLR2

The coding sequence of TLR2 was amplified by PCR using KOD FX DNA polymerase (TOYOBO) with a pair of oligonucletides, TLR2 exon 3-forward (5′-ATTAGAAT TACGATATGCTGTC-3′) and TLR2 exon 3-reverse (5′-ATGACGGTACATCCACGTAG-3′) as primers, essentially according to manufacturer's recommendations. Sequencing reaction was performed using BigDye® Terminators v1.1 Cycle Sequencing Kit (Applied Biosystems) and analyzed by ABI3730xl automated DNA sequencer (Applied Biosystems).

Transfection of TLR2 expression vectors

PCR products including the entire coding sequence of TLR2 were ligated to pGEM®-TEasy (Promega) with T4 DNA ligase after treatment with A-attachment Mix (TOYOBO). After the confirmation of nucleotide sequence

of plasmid clones, the DNA fragment containing entire coding region for TLR2 was isolated by cleavage with restriction enzymes and inserted to pcDNA3.1/Hygro(+) expression vector (Invitrogen). Luciferase reporter for nuclear factor kappa B (NF-κB) activity, pGL4.22-6xκB was constructed by inserting DNA fragment containing 6 times tandem repeats of NF-κB binding sequence and TATA box (Shibata et al. 2006) in pGL4.22[luc2CP/Puro] promoterless firefly luciferase reporter vector (Promega). All expression plasmid DNA and reporter plasmid DNA were prepared by Illustra™ Plasmid Prep Midi Flow kit (GE Healthcare) and confirmed virtually endotoxin free.

HEK293 cells were cultured in Dulbecco's MEM (Wako) supplemented with 10% fetal bovine serum (GIBCO) and 100 U/ml penicillin–100 μg/ml streptomycin (Invitrogen) at 37°C in the presence of 5% CO_2. Synthetic bacterial lipoproteins as TLR2 agonists, Pam2CSK4 and Pam3CSK4 were purchased from InvivoGen and applied at 10 and 100 ng/ml, respectively. Transfection of DNA was performed as follows: HEK293 cells were inoculated in 35-mm tissue culture dishes at 4×10^5 cells/dish on the previous day, transfected with a mixture of 250 ng of each pcDNA3.1-TLR2 expression plasmid, 100 ng of pGL4.22-6xκB, and 20 ng pRL-TK internal control (Promega) with FuGENE® HD Transfection Reagent (Roche), then at 42 h after the addition of DNA, stimulated with TLR2 agonists for 6 h. Cells were washed with 1 ml of PBS and suspended in 100 μl of 1× Passive Lysis Buffer (Promega). Luciferase activities were determined using Dual-Luciferase® Reporter Assay System (Promega) by Wallac 1420 Multilabel Counter ARVO MA (PerkinElmer). Transfection was set up in triplicate to evaluate experimental variations and repeated at least twice to confirm the results. Difference in luciferase activity was statistically examined by ANOVA and Student's *t* test.

Analysis of molecular evolution

We estimate values of the number of segregating sites (S), number of haplotypes (H), haplotype diversity (Hd), nucleotide diversities (π), nucleotide polymorphism (θ), K_a, K_s, K_a/K_s ratio, and Tajima's D (Tajima 1989) by using DnaSP ver.5.10.00 (Librado and Rozas 2009). Genetic distances for non-synonymous substitution (d_N) and synonymous substitution (d_S) and the d_N-d_S difference were calculated according to Nei and Gojobori's method (Nei and Gojobori 1986) with Jukes and Canter's correction by MEGA4 (Kumar et al. 2008). Z tests for positive and purifying selections were also carried out on MEGA4, by which standard errors were produced with 500 bootstrap replications. Results were considered statistically significant when $p<0.05$. A neighbor-joining tree (Saitou and Nei 1987) was constructed on the basis of genetic distances from alignments of the coding sequence of TLR2 alleles, estimated by Kimura's two-parameter method (Kimura 1980). Difference in frequencies of non-synonymous and synonymous substitutions was evaluated by Fisher's exact test (Zhang et al. 1998). Further, codon-wise evaluation for positive selection was conducted by employing statistical test implemented in PAML 4 package (Yang 2007) based on maximum likelihood estimation method.

Homology modeling of molecular structure of *Macaca* TLR2-TLR1

The optimal structures of macaque TLR2-TLR1 variants were determined by means of homology modeling algorithm implemented in Molecular Operation Environment (MOE) 2010.10 (Chemical Computing Group Inc, http://www.chemcomp.com/) using a template structure of human TLR2-TLR1 heterodimer bound with Pam3CSK4 (PDB accession # 2Z7X). The PDB data contained structural data for human TLR2 (27–506) and human TLR1 (25–475) fused to 67 amino acid-long peptide derived from inshore hagfish *Eptatretus* VLRB.61. The structure of ternary complex of human TLR2 (27–506)-human TLR1 (25–475) dimer and a lipopeptide ligand Pam3CSK4 was optimized after trimming of C-terminal fusion peptides. Molecular stability was expressed by the sum of potential energy between atoms in kcal/mol. Amino acid sequence of macaque TLR1 (25–475) was retrieved from GenBank accession # NM_001130424. London dG score, an index for affinity between receptor and ligand within the binding pocket, was obtained for each optimized complex structure by Lig-X algorithm suite implemented in MOE 2010.10.

Results

Identification of SNPs in TLR2 coding sequence from *M. mulatta* and *M. fuscata*

In the present study, nucleotide sequence of the 2,355-bp long entire coding region of TLR2 encoded within the third exon was determined for of 21 *M. mulatta* and 35 *M. fuscata* individuals. By the comparison of *M. mulatta* sequences, six non-synonymous and three synonymous substitutions were identified, while three non-synonymous and five synonymous substitutions were found in *M. fuscata* (Table 1; Fig. 1). One synonymous substitution, GTG(Val)>GTT(Val) at codon 373 was common to these two species. Further, all 21 *M. mulatta* individuals were homozygous for AAT(Asn) while all *M. fuscata* examined were homozygous for TAT(Tyr) at codon 326. Collectively, ten non-synonymous and seven synonymous substitutions were found in this population.

Table 1 Haplotype of 17 SNPs found in 21 *Macaca mulatta* and 35 *Macaca fuscata* individuals in the present study

Haplotype	Nucleotide position																
	93 Codon	292	570	664	703[a]	976[a]	1119[a]	1176	1214	1246	1359[a]	1507	1633	1667	1743	1908	2344
	31	98	190	222	235[a]	326[a]	373[a]	392	405	416	453[a]	503	545	556	581	636	782
M. mulatta (frequency in $2N$=42)																	
Mamu-Hap1 (17)	GAC (Asp)	TCC (Ser)	GAG (Glu)	AGT (Ser)	AAC (Asn)	AAT (Asn)	GTG (Val)	TTA (Leu)	ACC (Thr)	ACT (Thr)	GGC (Gly)	CTG (Leu)	ACT (Thr)	GCT (Ala)	TCA (Ser)	AAC (Asn)	ATA (Ile)
Mamu-Hap2 (10)	–	–	–	–	–	–	–	TTG (Leu)	–	–	–	GTG (Val)	–	–	–	–	–
Mamu-Hap3 (2)	–	–	–	–	–	–	–	–	–	GCT (Ala)	–	–	–	–	–	–	–
Mamu-Hap4 (2)	GAT (Asp)	–	–	–	–	–	–	TTG (Leu)	–	–	–	GTG (Val)	GCT (Ala)	–	–	–	–
Mamu-Hap5 (5)	–	–	–	–	–	–	–	–	–	–	–	GTG (Val)	–	–	–	–	–
Mamu-Hap6 (2)	–	–	–	–	–	–	–	–	–	–	–	GTG (Val)	–	GTT (Val)	–	–	–
Mamu-Hap7 (1)	–	–	–	–	–	–	GTT (Val)	–	ATC (Ile)	–	–	GTG (Val)	–	GTT (Val)	–	–	–
Mamu-Hap8 (1)	–	CCC (Pro)	–	–	–	–	–	–	–	–	–	GTG (Val)	–	–	–	–	–
Mamu-Hap9 (1)	–	–	–	–	–	–	–	–	–	–	–	GTG (Val)	GCT (Ala)	–	–	–	–
Mamu-Hap10 (1)	–	–	–	–	–	–	GTT (Val)	–	–	GCT (Ala)	–	–	–	–	–	–	–
M. fuscata (frequency in $2N$=70)																	
Mafu-Hap1 (50)	GAC (Asp)	TCC (Ser)	GAG (Glu)	AGT (Ser)	GAC (Asp)	TAT (Tyr)	GTT (Val)	TTA (Leu)	ACC (Thr)	ACT (Thr)	GGT (Gly)	CTG (Leu)	ACT (Thr)	GCT (Ala)	TCA (Ser)	AAC (Asn)	ATA (Ile)
Mafu-Hap2 (4)	–	–	GAA (Glu)	–	AAC (Asn)	–	GTG (Val)	–	–	–	GGC (Gly)	–	–	–	–	–	–
Mafu-Hap3 (1)	–	–	–	–	AAC (Asn)	–	GTG (Val)	–	–	–	GGC (Gly)	–	–	–	–	–	–
Mafu-Hap4 (2)	–	–	–	GGT (Gly)	–	–	–	–	–	–	–	–	–	–	TCG (Ser)	–	–
Mafu-Hap5 (5)	–	–	–	–	–	–	–	–	–	–	–	–	–	–	–	AAT (Asn)	–
Mafu-Hap6 (7)	–	–	–	GGT (Gly)	–	–	–	–	–	–	–	–	–	–	–	–	–
Mafu-Hap7 (1)	–	–	–	–	–	–	–	–	–	–	–	–	–	–	–	–	TTA (Leu)
Human[b]	GAC (Asp)	TCC (Ser)	GAG (Glu)	AGT (Ser)	GAC (Asp)	TAT (Tyr)	GTT (Val)	TTA (Leu)	ACC (Thr)	ACT (Thr)	GGT (Gly)	GTG (Leu)	ACT (Thr)	ATT (Ile)	TCA (Ser)	AGC (Ser)	ATA (Ile)

Polymorphic nucleotide in each codon is underscored. Frequency of haplotype appeared in the population is shown in parenthesis

[a] The positions where the major haplotypes for *M. mulatta* (Mamu-Hap1) and *M. fuscata* (Mafu-Hap1) are different from each other

[b] Only the human sequence (GenBank accession #NM_003264) corresponding to polymorphic codons among *Macaca* species are shown to tell whether is more probable to be ancestral between *Macaca* alleles

The extracellular domain of TLR2 is mainly composed with the leucine-rich repeat (LRR) modules and can be divided into three sub-domains; N-terminal, central, and C-terminal sub-domains with their unique β-sheet conformations (Fig. 1). The structure of extracellular domains of triacylated lipopeptide-bound TLR2-TLR1 heterodimer and those of diacylated lipopeptide-bound TLR2-TLR6 heterodimer has been revealed by X-ray diffraction analysis (Jin et al. 2007; Kang et al. 2009). Amino acid residues which contribute to the binding of ligands and the interaction to dimerization partner were mapped in the middle of extracellular domain. The distribution of polymorphic sites in terms of structural sub-domains was shown in Fig. 1. It is of note that the abovementioned inter-species substitution at codon 326, Asn in *M. mulatta* versus Tyr in *M. fuscata*, is located within ligand binding and dimerization domain for TLR2-TLR1 heterodimer which may contribute to certain functional properties (Fig. 1b).

Upon the inference of the combination of SNPs by PHASE program implemented in DnaSP package (see below), a major allele of *M. mulatta* population (Mamu-Hap1 in Table 1) was obtained. Mamu-Hap1 had four nucleotide substitutions, GTT(Val)>GTG(Val) at codon 373, ATC (Ile)>ACC(Thr) at codon 405, GTG(Val)>CTG (Leu) at codon 503 and GTT(Val)>GCT(Ala) at codon 556, from the *M. mulatta TLR2* sequence reported previously, GenBank accession #AB445630 (Nakajima et al. 2008), which is identical to Mamu-Hap7 in the present study. The homology between *M. mulatta* and humans is 97.2% (2,289/2,355 bp) at nucleotide level and 95.8% (751/784) at amino acid level. Because general homology in nucleotide sequences between *M. mulatta* and humans is 93.94% identical in average (Rhesus Macaque Genome Sequencing and Analysis Consortium 2007), TLR2 is one of the well-conserved genes during primate evolution. A major allele of *M. fuscata* (Mafu-Hap1 in Table 1) was also inferred (GenBank accession, #AB607964) and had four nucleotide substitutions from Mamu-Hap1: AAC(Asn)>GAC(Asp) at codon 235, AAT(Asn)>TAT(Tyr) at codon 326, GTG(Val)>GTT(Val) at codon 373 and GGC(Gly)>GGT(Gly) at codon 453. Another less-frequent Mafu-Hap3 had only one substitution, AAT(Asn)>TAT(Tyr) at codon 326 from Mamu-Hap1. Figure 2 explains genealogy of allelic variants. Intra-specific variants are connected by as many as five and six mutation events in *M. mulatta* and *M. fuscata*, respectively, while Mamu-Hap1 and Mafu-Hap3 differ by one nucleotide substitution as mentioned above. In addition, a synonymous substitution at codon 373 was

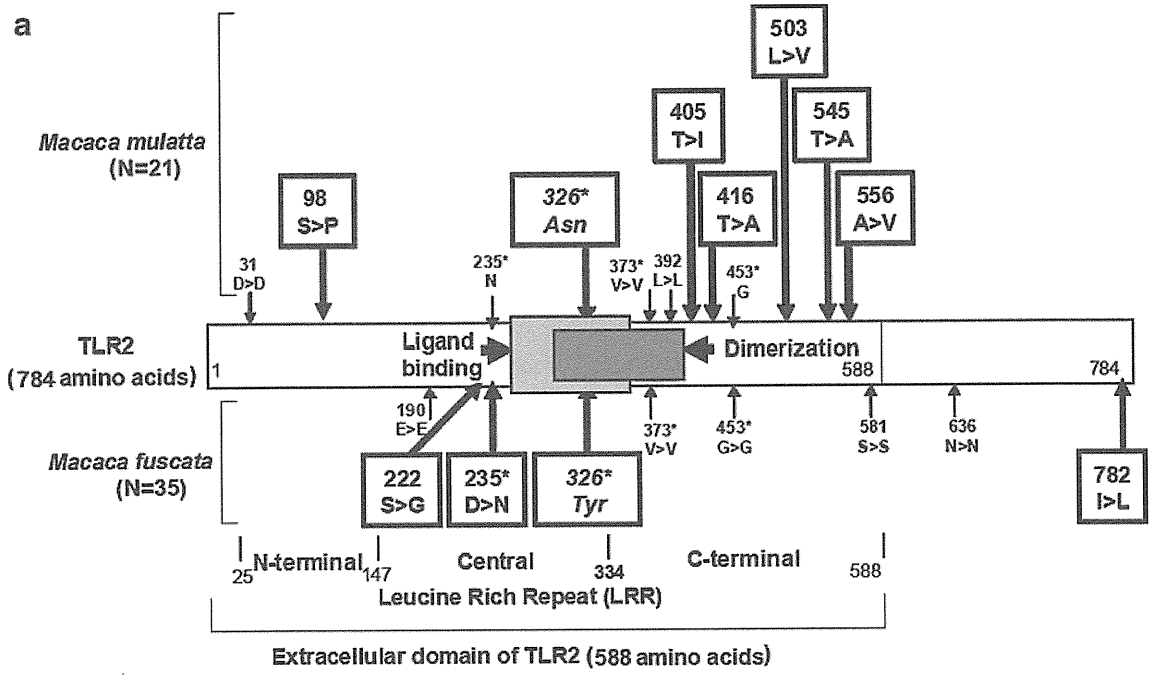

Fig. 1 The distribution of SNPs found in *M. mulatta* and *M. fuscata* populations. **a** The position of codons with synonymous (*plain*) and non-synonymous (*boxed*) SNPs is shown in schematic representation of TLR2; SNPs in *M. mulatta* and *M. fuscata* populations are the upper and the lower halves, respectively. Domain and sub-domain structures are also illustrated. The regions contributing to ligand binding (codon 266–359) and interaction with dimerization partner (codon 318–398 for TLR2-TLR1 and codon 318–404 for TLR2-TLR6) are depicted as overlapping *filled boxes* in the middle of extracellular domain (Jin et al. 2007; Kang et al. 2009). **b** Structure and amino acid sequence of TLR2. Leucine-rich domain (LRR)s at N terminus, #1 to #20 and at C terminus, and transmembrane and cytoplasmic regions (*TM+CY*) are shown above the sequence. Amino acid residues involved in ligand binding (*l*) and dimerization interface (*i*) are indicated. Sequence variations between human and *M. mulatta* (*asterisk*), among *M. mulatta* and among *M. fuscata* (var. site) are also indicated

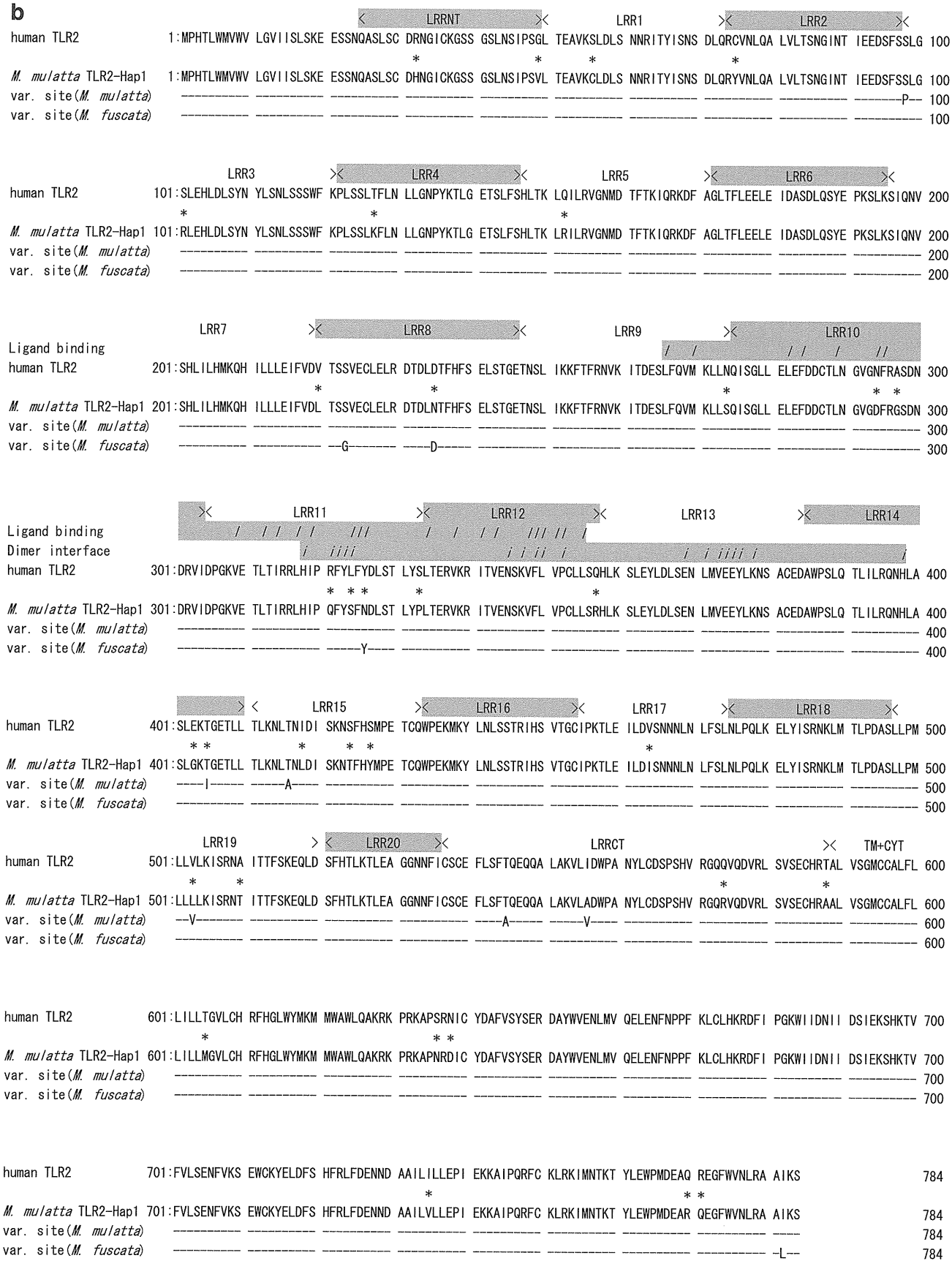

Fig. 1 (continued)

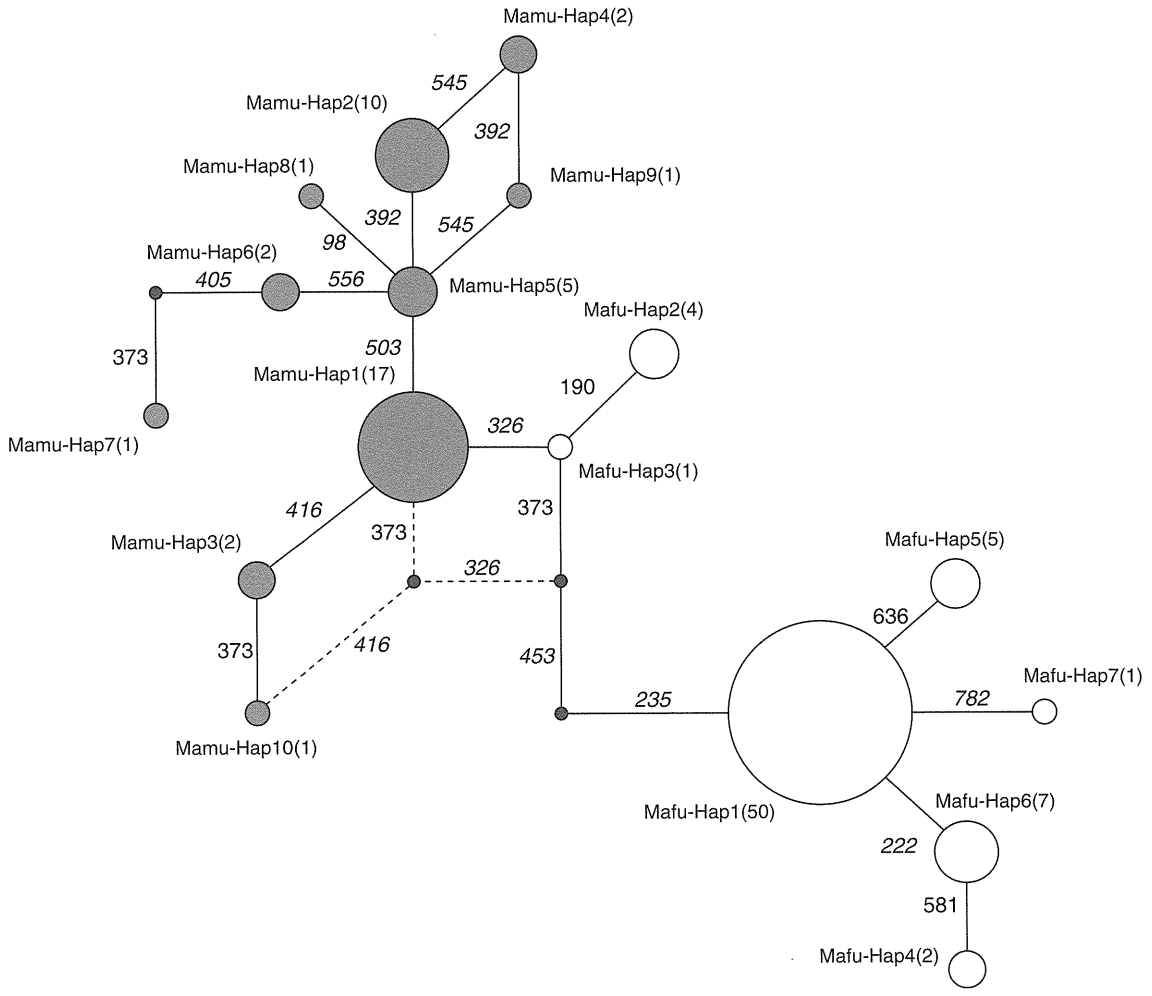

Fig. 2 Genealogical relationship of *Macaca* TLR2 alleles. A genealogical pathway of allelic variants is illustrated by network. *Gray* and *open circles* are allelic variants of *M. mulatta* and *M. fuscata* TLR2, respectively. Two variants differ by one nucleotide substitution are connected by *bar*. *Numbers near the bars* are codon positions; non-synonymous substitution is shown in *italic* style. Intra-specific variants are connected by as many as five and six mutation events in *M. mulatta* and *M. fuscata*, respectively, while Mamu-Hap1 and Mafu-Hap3 differ by one nucleotide substitution. It is of note that a synonymous substitution at codon 373 is commonly found in two species

commonly found in two species. Thus the difference between variants across the species is not more than the maximal difference within a species for certain combinations.

Molecular evolution of TLR2

In order to evaluate the allelic divergence of *Macaca TLR2* locus, we applied PHASE program to infer the haplotypes of 17 SNPs observed in two *Macaca* species. Consequently, ten haplotypes for *M. mulatta* and seven haplotypes for *M. fuscata* were identified (Table 1). Presence of these haplotypes was confirmed by nucleotide sequencing of plasmid clones. A phylogenetic tree (Fig. 3) was drawn by neighbor-joining method according to sequence alignments shown in Table 1. Because of amino acid substitution at codon 326, alleles of *M. mulatta* and *M. fuscata* were positioned in two separate lineages.

S, *H*, *Hd*, π, θ, average codon-based evolutionary divergence (d_S, d_N, and d_N, d_S), and Tajima's D were calculated for overall and sub-domains of *M. mulatta* and *M. fuscata* TLR2 (Table 2). Sliding window plots for Tajima's D value for each species and K_a/K_s ratio between two species are also presented (Figs. 4 and 5). When the statistical significance was examined by *Z* test, the entire TLR2 coding sequence of *M. fuscata* gave a significant result with a codon-based test (d_N, d_s) for purifying selection (p=0.0435), whereas became not significant if the extracellular domain was separately examined (p= 0.061). But further breaking down of the extracellular domain into three parts, C-terminal LRR domain underwent purifying selection by codon-based test (p=0.0406). In contrast, a part of the extracellular domain C-terminal to ligand binding and dimerization domain of *M. mulatta* TLR2 was rich in non-synonymous substitutions with a

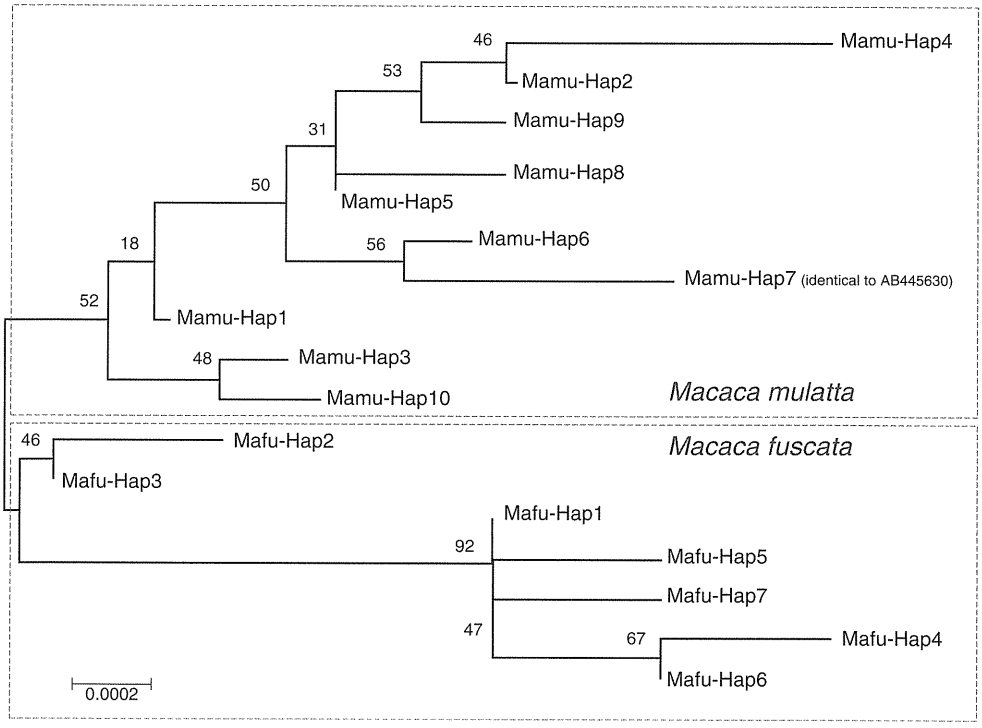

Fig. 3 Phylogenetic tree for *Macaca* TLR2 alleles. A phylogenetic tree is drawn by neighbor-joining method based on a distance matrix of Kimura's two-parameter evolutional model using MEGA4.0.2. Bootstrap percent probability for 500 replications is shown at each node. The *scale bar* represents a genetic distance of 0.0002

significant result for codon-based test for positive or diversifying selection (p=0.0362). Sliding window plot of Tajima's D for *M. mulatta* TLR2 (Fig. 4a) shows clearly different pattern from that of *M. fuscata* TLR2 (Fig. 4b): the N terminus of *M. mulatta* TLR2 and the membrane-proximal region of extracellular domain of *M. fuscata* TLR2 exhibit weak tendency of purifying selection because of the presence of synonymous substitutions, while the membrane-proximal region of extracellular domain of *M. mulatta* TLR2 shows positive D value suggesting the operation of positive selection. When all sequence of two species ($2N$=42 for ten *M. mulatta* variants and $2N$=70 for seven *M. fuscata* variants) were taken into account, average codon-based evolutionary divergence indicated by the value of K_a/K_s ratio is highest in the part of central LRR, mostly attributed to amino acid substitution at codon 326 (Table 3) while two peaks of K_a/K_s ratio corresponding to the central LRR and the amino acid substitutions in the membrane-proximal part of extracellular domain of *M. mulatta* TLR2 appear when the sliding window is narrowed to 350-bp range (Fig. 5). When the frequency of non-synonymous substitution in possible sites (five in 387) within in the membrane-proximal part of extracellular domain (codon 401 to 566) of *M. mulatta* TLR2 was compared with that of synonymous substitution (0 in 111), they were not significantly different (p=0.358; Table 4, comparison A), but the number of non-synonymous substitutions is over-represented in *M. mulatta* than *M. fuscata* (5 vs. 0) in comparison to that of synonymous substitutions (0 vs.2) within the same region (p=0.048; Table 4, comparison B), suggesting the presence of differential selection pressure on these two species. Further, codon-wise evaluation for non-synonymous and synonymous substitutions was conducted for extracellular domain of *M. mulatta* TLR2 by employing statistical test implemented in PAML 4 package based on maximum likelihood estimation method. Likelihood statistics under different molecular evolution models were presented in Table 5. By comparison of likelihoods between neutral and selection site models, we could obtain a weak but significant signal for positive selection at codon position 545. This position is not known to be involved in ligand binding or dimerization interface in the diacylated lipoprotein-bound structure of TLR2-TLR6 dimer or the triacylated lipoprotein-bound structure of TLR2-TLR1 dimer (Fig. 1b).

Functional analysis for TLR2 alleles

In order to clarify whether amino acid substitutions in *Macaca* TLR2 alleles can bring any functional alteration, an experimental system was designed to measure the downstream transcriptional activation of NF-κB-dependent synthetic enhancer-promoter upon the stimulation with TLR2 agonists. It is of importance to examine functional integrity of variants to rule out pseudogenization of TLR-2 in *Macaca* lineage as one of possible cause of rapid accumulation of non-synonymous mutations. We chose HEK293 cells as recipients of DNA transfection assay because it has been proven to be lower intrinsic TLR2

Table 2 Polymorphism and nucleotide diversity in the coding sequence of TLR2 locus

Domain[a]	Range (bp)	*S*	*H*	*Hd*	π ($\times 10^{-4}$)	θ ($\times 10^{-4}$)	d_S (±SE)	d_N (±SE)	d_N-d_S (±SE)	Tajima's D
Macaca mulatta (*n*=21)										
Total	1–2,355	9	10	0.775	6.9	8.9	0.0011±0.0008	0.0006±0.0003	−0.0006±0.0008	−0.65546
Extracellular	1–1,764	9	10	0.775	9.2	11.9	0.0015±0.0010	0.0007±0.0004	−0.0008±0.0011	−0.65546
N-terminal LRR	73–438	2	3	0.138	3.8	12.7	0.0010±0.0010	0.0002±0.0002	−0.0009±0.0011	−1.30048
Central LRR	439–999	0	1	0.000	0.0	n.d.	0.0000±0.0000	0.0000±0.0000	0.0000±0.0000	n.d.
C-terminal LRR	1,000–1,764	7	9	0.769	19.3	21.3	0.0029±0.0024	0.0016±0.0009	−0.0013±0.0027	−0.25176
N-terminal part	1–795	2	3	0.138	1.8	5.8	0.0005±0.0005	0.0001±0.0001	−0.0004±0.0005	−1.30048
Lig-bind/dimer	796–1,194	2	3	0.483	12.8	11.6	0.0057±0.0048	0.0000±0.0000	−0.0057±0.0046	0.18543
C-terminal part	1,195–1,764	5	6	0.695	17.0	20.4	0.0000±0.0000	0.0022±0.0012	0.0022±0.0012*	−0.42381
TM-Cyt	1,765–2,355	0	1	0.000	0.0	n.d.	0.0000±0.0000	0.0000±0.0000	0.0000±0.0000	n.d.
Macaca fuscata (*n*=35)										
Total	1–2,355	8	7	0.477	4.1	7.0	0.0011±0.0005	0.0002±0.0001	−0.0009±0.0005**	−1.08369
Extracellular	1–1,764	6	5	0.351	4.5	7.1	0.0011±0.0005	0.0003±0.0002	−0.0008±0.0006	−0.85999
N-terminal LRR	73–438	0	1	0.000	0.0	n.d.	00000±0.0000	0.0000±0.0000	0.0000±0.0000	n.d.
Central LRR	439–999	3	4	0.345	8.4	11.1	0.0009±0.0009	0.0008±0.0006	0.0000±0.0010	−0.46715
C-terminal LRR	1,000–1,764	3	3	0.187	4.3	8.1	0.0019±0.0011	0.0000±0.0000	−0.0019±0.0011***	−0.91696
N-terminal part	1–795	3	4	0.345	5.9	7.8	0.0006±0.0006	0.0006±0.0004	0.0000±0.0007	−0.46715
Lig-bind/dimer	796–1,194	1	2	0.135	3.4	5.2	0.0015±0.0015	0.0000±0.0000	−0.0015±0.0015	−0.43152
C-terminal part	1,195–1,764	2	3	0.187	3.3	7.3	0.0015±0.0011	0.0000±0.0000	−0.0015±0.0012	−0.89232
TM-Cyt	1,765–2,355	2	3	0.161	2.8	7.0	0.0011±0.0010	0.0001±0.0001	−0.0010±0.0011	−1.00276

S number of variable sites, *H* number of haplotypes, *Hd* haplotype diversity, π nucleotide diversity (per site), θ nucleotide polymorphism (per site), d_S number of synonymous substitutions per site, d_N number of non-synonymous substitutions per site, d_N-d_S difference between the non-synonymous and synonymous distances per site; Tajima's D: Tajima's D statistic

*p=0.0362 upon Z test for positive (or diversifying) selection; *p=0.0435; *p=0.0406 upon Z test for purifying selection

[a] 2,355-bp of total open reading frame for TLR2 is divided to extracellular domain and the rest (TM-Cyt: transmembrane and cytoplasmic). Extracellular domain is further broken down to three sub-domains in two ways: one according to the differential motifs of leucine-rich repeats (LRR) and the other according to structural analysis of TLR2-TLR1 heterodimeric complex (Jin et al. 2007) delineating the region contributes to ligand binding and interaction to dimerization partner (Lig-bind/Dimer)

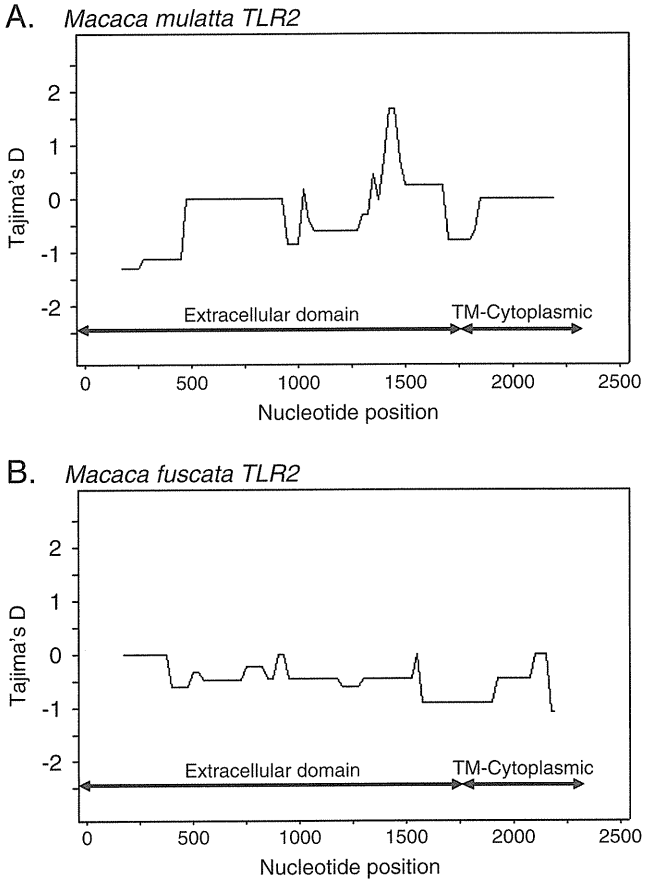

Fig. 4 Distribution of polymorphisms evaluated by Tajima's D statistic. Sliding window plots of Tajima's D with 350 bp window and 25-bp steps are drawn for *M. mulatta* (**a**) and *M. fuscata* (**b**) *TLR2* using DnaSP ver5.10.00. Although Tajima's D does not reach to significant levels, it tends to be below zero in general

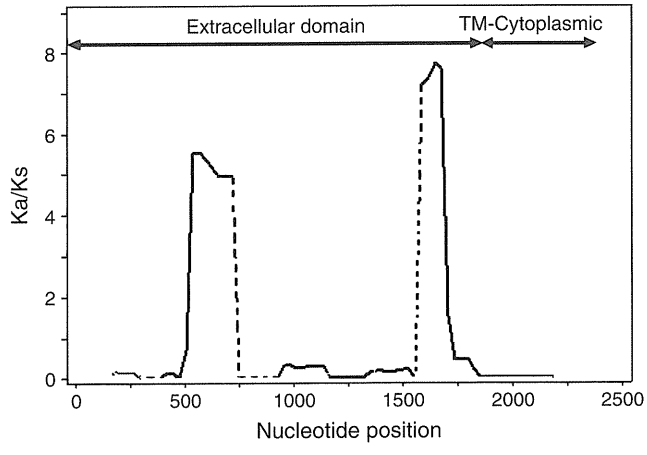

Fig. 5 Distribution of non-synonymous substitutions in two *Macaca* species. A sliding window plot of K_a/K_s ratio between *M. mulatta* and *M. fuscata* alleles with 350 bp window and 30-bp steps is drawn using DnaSP ver5.10.00. *Dotted lines* show the parts where the K_a/K_s ratio is not obtained because of the absence of synonymous substitutions

Table 3 Estimation of rate of synonymous and non-synonymous substitutions between *Macaca mulatta* and *Macaca fuscata*

Domain[a]	Range (bp)	K_s	K_a	K_a/K_s
Total	1–2,355	0.00435	0.00157	0.359
Extracellular	1–1,764	0.00553	0.00209	0.377
N-terminal LRR	73–438	0.00053	0.00009	0.164
Central LRR	439–999	0.00046	0.00471	10.312
C-terminal LRR	1,000–1,764	0.01221	0.00129	0.105
TM-Cyt	1,765–2,355	0.00057	0.00003	0.054

K_s synonymous nucleotide divergence, K_a non-synonymous nucleotide divergence, K_a/K_s the ratio of K_a to K_s

[a] See footnote of Table 2

activity and to possess the other components necessary for TLR2-mediated, ligand-induced transcriptional activation (Schwandner et al. 1999). When the expression plasmid for a major allele of *M. mulatta* TLR2, Mamu-Hap1 was introduced to HEK293 cells, two synthetic TLR2 ligands, Pam2CSK4 and Pam3CSK4, which are relatively specific to TLR2-TLR6 and TLR2-TLR1 heterodimers, respectively, could induce very strong luciferase activity to almost equivalent extent to human TLR2 expression plasmid (Fig. 6a). Therefore, the function of *M. mulatta* TLR2 in combination with HEK293-intrinsic TLR6 and TLR1 remains intact in the presence of mutations taken place after the species diversification, indicating the higher rate of amino acid substitutions observed in *M. mulatta* lineage are not attributable to pseudogenization. Further, the effect of amino acid substitution at codon 326 was evaluated by the comparison between Mamu-Hap1 and Mafu-Hap3, obtaining no evidence for functional relevance to the substitution by this experimental system (Fig. 6b). Further, the effect of all six non-synonymous substitutions found in *M. mulatta* population was examined by using four additional expression plasmids: Mamu-Hap3 carrying Ala416, Mamu-Hap7 carrying Ile405-Val503-Val556, Mamu-Hap8 carrying Pro98-Val503, and Mamu-Hap9 carrying Val503-Ala545 (Fig. 6c). Although Pam3CSK4-induced luciferase activity was higher for Mamu-Hap8 than Mamu-Hap7 and Mamu-Hap9, statistic obtained by ANOVA, by which the inflation of statistical error by multiplicity of comparison is taken into account, did not reach to significance. Thus, we could not demonstrate any functional augmentation or deterioration accompanied with seven non-synonymous amino acid substitutions identified in the present study.

Structural analysis by computational chemistry

The non-synonymous substitution at codon position 326 appeared to be differentially fixed in each species, asparagine for *M. mulatta* whereas tyrosine for *M. fuscata*.

Table 4 Comparison of frequencies of non-synonymous and synonymous substitutions in proximal region (amino acid positions, 401–566) of extracellular domain of TLR2

	Non-synonymous	Synonymous	Total	*P* value (Fisher's exact test)
Comparison A: test for difference in frequencies of non-synonymous and synonymous changes in *Macaca mulatta TLR2*				
Changes SNPs)	5	0	5	0.358
No changes	382	111	493	
Total	387	111	498 (nucleotide positions, 1,201–1,698)	
Comparison B: comparison of number of SNPs in *M. mulatta* and *Macaca fuscata TLR2*				
M. mulatta	5	0	5	0.048
M. fuscata	0	2	2	
Total	5	2	7	

The change may contribute to certain functional properties, because it locates in the region contributing to ligand binding and interaction with dimerization partner of TLR2-TLR1 heterodimeric complex (Fig. 1a). Homology modeling was applied to determine the most stabilized structure for macaque TLR2-TLR1 dimers composed of different TLR2 variants. Because of the sequence conservation across primates including human, Tyr326 (*M. fuscata* type) is assumed to be ancestral and Asn326 (*M. mulatta* type) is derivative. The effect of single amino acid substitution at position 326 was evaluated by the comparison between Mamu-Hap1 and Mafu-Hap3 (Table 6, Supplementary figures 1 and 2). Relative binding affinity to Pam3CSK4 is attenuated by approximately 5% by amino acid substitution Tyr>Asn (100.0>94.5 Table 6), which is elucidated by structural change in ligand binding pocket composed of TLR2-TLR1 dimer in part (Supplementary Figures 1 and 2). The affinity to ligand is partially recovered by second substitutions in the membrane-proximal region of extracellular domain of TLR2 (Table 6), although these substitutions were not directly involved in ligand binding or dimerization with the TLR1 partner but were supposed to induce subtle change in intra-chain interaction of TLR2 (Supprementary Figures 3 and 4).

Discussion

The rhesus monkey, *M. mulatta* has been applied to many biomedical researches for a long time, because it provides a better relevance of model organism to humans in many pathological and physiological aspects. While the lack of inbred strains or closed colony with great animals is a drawback for the use of experimental model because of variations in biological response based on underlying genetic diversity, it turns to an advantage once the genetic variations are fully understood and are controlled adequately (Matano et al. 2004). Recently, complete genome of *M. mulatta* has

Table 5 Log-likelihood values and parameter estimates under different codon substitution models for ten *Macaca mulatta* TLR2 allelic variants

Model	Number of parameters	*l*: ln(likelihood)	Average ω (d_N/d_S)	Estimates of parameters
One ratio (M0)	1	−2,461.85	0.777	ω=0.777
Site-specific models				
M1a: neutral	2	−2,461.42	0.530	p_0=0.47 (p_1=1–p_0=0.53), ω_0=0.00
M2a: selection	4	−2,458.36	0.781	p_0=0.963, p_1=0 (p_2=1–p_0–p_1=0.037), ω_0=0.00, ω_2=21.29
M3: discrete	5	−2,458.36	0.782	p_0=0.002, p_1=0.961 (p_2=1–p_0–p_1=0.037), ω_0=0.00, ω_1=0.00, ω_2=21.30
M7: beta	2	−2,460.40	0.500	p=0.0074, q=0.0073
M8: beta and ω	4	−2,458.36	0.782	p_0=0.963, p=0.0050, q=4.116 (p_1=1–p_0=0.037), ω_s=21.30
Comparisons				
One ratio (M0) vs. discrete (M3)	χ^2=−2Δ*l*=6.98	*df*=4	*p*=0.14	
Neutral (M1a) vs. selection (M2a)	χ^2=−2Δ*l*=6.12	*df*=2	*p*=0.047	
Beta (M7) vs. beta and ω (M8)	χ^2=−2Δ*l*=4.08	*df*=2	*p*=0.13	

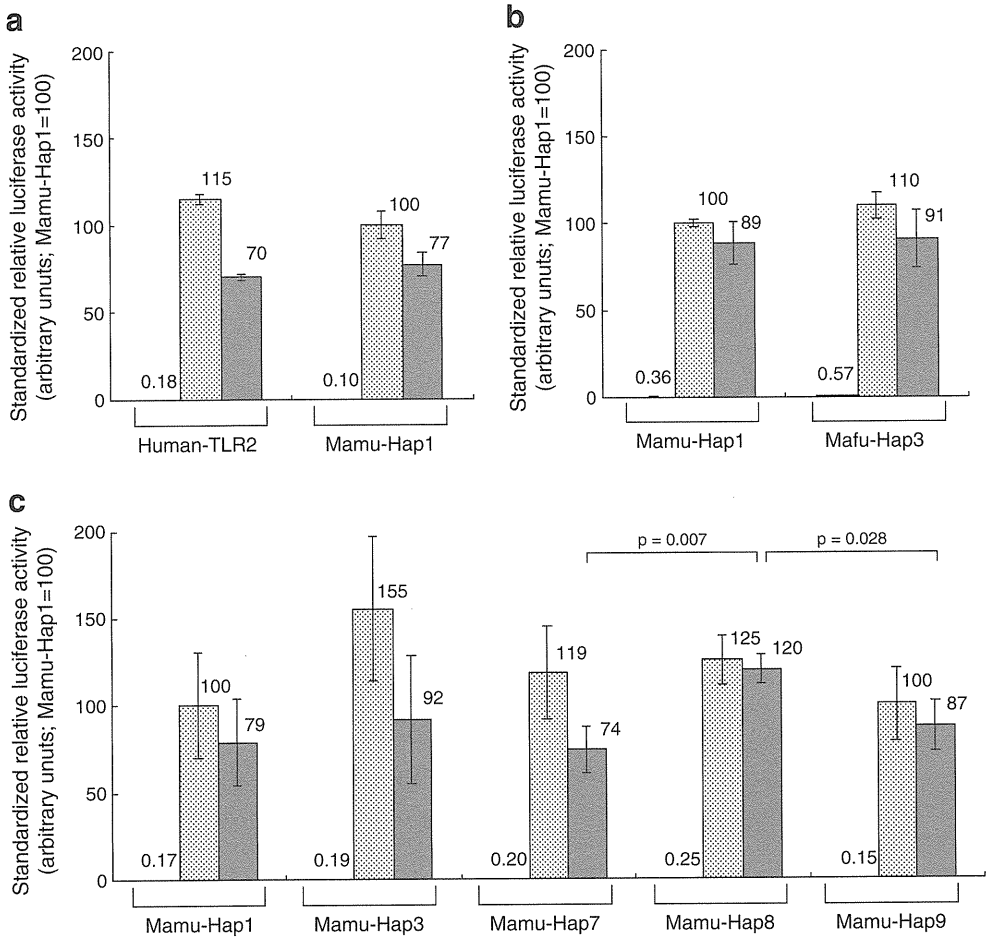

Fig. 6 Functional analysis of TLR2 alleles by luciferase reporter gene assay. Relative luciferase activity of each triplicate transfection is obtained as the ratio of relative light units (*RLUs*) of firefly luciferase assay (for NF-κB-dependent activity) to RLUs of *Renilla* luciferase assay (for constitutive basal transcriptional activity) and standardized by the mean value of those of triplicate Mamu-Hap1 transfections to be 100 for respective experiments. The results of representatives of repeated experiments at least two times are shown. Mean value of triplicate standardized relative luciferase activities without TLR2 ligand (*left*) that with 10 ng/ml of Pam2CSK4 (*middle*, *stippled bar*) and that with 100 ng/ml of Pam3CSK4 (*right*, *filled bar*) are depicted as *bar gragh with whiskers* of SEM. **a** A major allele of *M. mullata*, Mamu-Hap1, brought almost equivalent activities to the human TLR2. **b**, **c** *Macaca* TLR2 alleles carrying Tyr326 (Mafu-Hap3), Ala416 (Mamu-Hap3), Ile405-Val503-Val556 (Mamu-Hap7), Pro98-Val503 (Mamu-Hap8), and Val503-Ala545 (Mamu-Hap9) substitutions were compared

been uncovered (Rhesus Macaque Genome Sequencing and Analysis Consortium 2007), and efforts to reveal genetic polymorphism of this species have been carried out (Singh and Schmidtke 2005; Ferguson et al. 2007; Karl et al. 2008; Flynn et al. 2009; Blokhuis et al. 2009). On the other hand, the Japanese monkey, *M. fuscata*, an endemic species of Japan, also draws an attention of investigators as experimental models to human pathophysiology (Kawai et al. 1993; Isa et al. 2009). *M. mulatta* and *M. fuscata* are very close to each other in terms of species diversification (Smith et al. 2007), but geographic isolation and differential influence of dwelling environment cause species-specific characteristic through evolution. For example, *M. fuscata* is extremely labile to cerebral involvement of monkey malaria in comparison to tropical *Macaca* species (Kawai et al. 1993), presumably because of the absence of circulation of *Plasmodium* protozoa in wild *M. fuscata* population. It is suggested that the origin of current species belonging to genus *Macaca* had emerged in northern part of African continent, migrated through the Middle-East into India, and settled in Asian continent and islands (Hernandez et al. 2007). The population history of migration out of Africa and settlement in their destinations is very similar to that of divergent human ethnic groups. Infectious diseases such as malaria and arthropod-borne viral hemorrhagic fever would be a heavy burden to thrive in the tropical region in *Macaca* species as well as humans. Therefore, comparative studies of different *Macaca* species would provide valuable clues for the better understanding of host defense mechanisms of these species as well as those of humans against various infectious agents.

The previous studies on primate TLR genes revealed that the cytoplasmic TIR domains of *M. mulatta* TLRs shares high

Table 6 Molecular stability and interaction energy estimated for TLR ternary complex structure obtained by optimization through homology modeling

Ternary complex of TLR dimer and ligand	Total energy[a] (kcal/mol)	Ligand[b] (kcal/mol)	Interaction[c] (kcal/mol)	London dG score[d] (kcal/mol)	Relative affinity to ligand (macaque TLR2(Tyr326)=100)
Human TLR2 (27–506)-TLR1(25–475)-Pam3CSK4[e]	−11,680.30	−393.12	−110.59	−26.21	105.6
Macaque TLR2(Tyr326)-TLR1-Pam3CSK4 (*M. fuscata*, hap-3)	−9,101.94	−398.09	−110.41	−24.81	100.0 (reference)
Macaque TLR2(Asn326)-TLR1-Pam3CSK4 (*Macaca mulatta*, hap-1)	−9,114.51	−397.85	−109.13	−23.52	94.5
Macaque TLR2(Asn326-Ile405)-TLR1-Pam3CSK4	−9,808.11	−396.92	−110.80	−24.24	97.7
Macaque TLR2(Asn326-Ala416)-TLR1-Pam3CSK4	−9,524.80	−399.36	−109.04	−24.46	98.6

[a] Total potential energy between all the atoms of extracellular domains of TLR2-TLR1 heterodimeric receptor (position 27–506 of TLR2 and position 25–475 of TLR1) and a ligand Pam3CSK4 was calculated by Molecular Operating Environment (MOE) 2010.10(Chemical Computing Group Inc)

[b] Total potential energy between all the atoms of Pam3CSK4

[c] Total potential energy between the atoms of TLR2-TLR1 heterodimeric receptor and those of Pam3CSK4

[d] An index for affinity between receptor and ligand within the binding pocket obtained by Lig-X algorithm suite implemented in MOE 2010.10

[e] Molecular structure was optimized by MOE 2010.10 after retrieval of PDB data accession# 2Z7X (available at RCSB, http://www.rcsb.org/pdb/) and trimming of C-terminal 67 residues of fusion peptide derived from inshore hagfish Eptatretus VLRB.61

levels of homology with human counterparts (Sanghavi et al. 2004), and TIR domains of TLRs and other related genes had undergone purifying selection among seven primate species (Nakajima et al. 2008), by which the presence of strict functional constraint is suggested. On the other hand, it was also revealed that the extracellular domain of *Macaca* TLR4 have been uniquely evolved under the diversifying selection by comparison between primate species (Nakajima et al. 2008). While the coding polymorphisms in *M. mulatta TLR4* and *TLR5* (Ferguson et al. 2007), as well as microsatellite located in the second intron of *TLR2* (Yim et al. 2006), were reported, we investigated for the first time SNPs in the coding region of *TLR2* for *M. mulatta* and *M. fuscata* individuals and reach to the trace evidence for differential purifying and diversifying selections on certain parts of extracellular domain in the present study. It is of note that the shapes of sliding window plots of Tajima's D (Fig. 4) were quite different between *M. mulatta* and *M. fuscata* suggesting differential molecular evolution for these species after species diversification. Inter-specific differential molecular evolution is also prominent in the sliding window plot of K_a/K_s ratio for combined *M. mulatta* and *M. fuscata* allelic variants (Fig. 5). Further, we could obtain a trace of positive selection at one amino acid position 545 by application of maximal likelihood estimation for codon-wise evaluation of molecular evolution events. Certain polymorphisms located in extracellular domain of swine *TLR2* (Shinkai et al. 2006; Bergman et al. 2010) and those of bovine *TLR2* (Jann et al. 2008) were also suggested to have been under positive selection during the domestication and breeding of these mammalian species. It is probable that positive selection has been driven by the functional alteration adapting to the changes of dwelling environments. Further, one of several rare variants of human TLR2, Thr411Ile, which has been shown functionally deteriorated upon the Pam3CSK4-induced, NF-κB-driven reporter gene assay (Merx et al. 2007; Kormann et al. 2009), is located in the part C-terminal to the ligand binding and dimerization domain in the vicinity of membrane-proximal region where five of the non-synonymous substitutions were found in our *M. mulatta* population. Although we could not demonstrate apparent augmentation or deterioration accompanied with amino acid substitutions in *M. mulatta* alleles by luciferase reporter gene assay using HEK293 cells as recipients with saturating doses of lipopeptide ligands in the present study, the affinity to ligand appeared different and would be differentially tuned during the evolution of two *Macaca* species under distinct environmental selection pressure.

Acknowledgments This work was supported in part by Japan Initiative for Global Research Network on Infectious Diseases (J-GRID) and the Global Centers of Excellence Program of the Ministry of Education, Culture, Sports, Science and Technology of Japan and by the Cooperation Research Program of Primate Research Institute, Kyoto University, Japan

References

Akira S, Uematsu S, Takeuchi O (2006) Pathogen recognition and innate immunity. Cell 124(4):783–801

Baena A, Mootnick AR, Falvo JV, Tsytskova AV, Ligeiro F, Diop OM, Brieva C, Gagneux P, O'Brien SJ, Ryder OA, Goldfeld AE

(2007) Primate TNF promoters reveal markers of phylogeny and evolution of innate immunity. PLoS One 2:e621

Bergman IM, Rosengren JK, Edman K, Edfors I (2010) European wild boars and domestic pigs display different polymorphic patterns in the Toll-like receptor (TLR) 1, TLR2, and TLR6 genes. Immunogenetics 62:49–58

Blancher A, Bonhomme M, Crouau-Roy B, Terao K, Kitano T, Saitou N (2008) Mitochondrial DNA sequence phylogeny of 4 populations of the widely distributed cynomolgus macaque (*Macaca fascicularis fascicularis*). J Hered 99:254–264

Blokhuis JH, van der Wiel MK, Doxiadis GG, Bontrop RE (2009) Evidence for balancing selection acting on KIR2DL4 genotypes in rhesus macaques of Indian origin. Immunogenetics 61:503–512

Bochud PY, Hawn TR, Aderem A (2003) A Toll-like receptor 2 polymorphism that is associated with lepromatous leprosy is unable to mediate mycobacterial signaling. J Immunol 170:3451–3454

Ferguson B, Street SL, Wright H, Pearson C, Jia Y, Thompson SL, Allibone P, Dubay CJ, Spindel E, Norgren RB Jr (2007) Single nucleotide polymorphisms (SNPs) distinguish Indian-origin and Chinese-origin rhesus macaques (*Macaca mulatta*). BMC Genomics 8:43

Flynn S, Satkoski J, Lerche N, Kanthaswamy S, Smith DG (2009) Genetic variation at the TNF-alpha promoter and malaria susceptibility in rhesus (*Macaca mulatta*) and long-tailed (*Macaca fascicularis*) macaques. Infect Genet Evol 9:769–777

Hayasaka K, Fujii K, Horai S (1996) Molecular phylogeny of macaques: implications of nucleotide sequences from an 896-base pair region of mitochondrial DNA. Mol Biol Evol 13:1044–1053

Hernandez RD, Hubisz MJ, Wheeler DA, Smith DG, Ferguson B, Rogers J, Nazareth L, Indap A, Bourquin T, McPherson J, Muzny D, Gibbs R, Nielsen R, Bustamante CD (2007) Demographic histories and patterns of linkage disequilibrium in Chinese and Indian rhesus macaques. Science 316:240–243

Huang D, Qiu L, Wang R, Lai X, Du G, Seghal P, Shen Y, Shao L, Halliday L, Fortman J, Shen L, Letvin NL, Chen ZW (2007) Immune gene networks of mycobacterial vaccine-elicited cellular responses and immunity. J Infect Dis 195:55–69

Isa T, Yamane I, Hamai M, Inagaki H (2009) Japanese macaques as laboratory animals. Exp Anim 58:451–457

Jann OC, Werling D, Chang JS, Haig D, Glass EJ (2008) Molecular evolution of bovine Toll-like receptor 2 suggests substitutions of functional relevance. BMC Evol Biol 8:288

Jin MS, Kim SE, Heo JY, Lee ME, Kim HM, Paik SG, Lee H, Lee JO (2007) Crystal structure of the TLR1-TLR2 heterodimer induced by binding of a tri-acylated lipopeptide. Cell 130:1071–1082

Kang JY, Nan X, Jin MS, Youn SJ, Ryu YH, Mah S, Han SH, Lee H, Paik SG, Lee JO (2009) Recognition of lipopeptide patterns by Toll-like receptor 2-Toll-like receptor 6 heterodimer. Immunity 31:873–884

Karl JA, Wiseman RW, Campbell KJ, Blasky AJ, Hughes AL, Ferguson B, Read DS, O'Connor DH (2008) Identification of MHC class I sequences in Chinese-origin rhesus macaques. Immunogenetics 60:37–46

Kawai S, Aikawa M, Kano S, Suzuki M (1993) A primate model for severe human malaria with cerebral involvement: *Plasmodium coatneyi*-infected *Macaca fuscata*. Am J Trop Med Hyg 48:630–636

Kimura M (1980) A simple method for estimating evolutionary rates of base substitutions through comparative studies of nucleotide sequences. J Mol Evol 16:111–120

Kormann MS, Ferstl R, Depner M, Klopp N, Spiller S, Illig T, Vogelberg C, von Mutius E, Kirschning CJ, Kabesch M (2009) Rare TLR2 mutations reduce TLR2 receptor function and can increase atopy risk. Allergy 64:636–642

Kumar S, Hedges SB (1998) A molecular timescale for vertebrate evolution. Nature 392:917–920

Kumar S, Nei M, Dudley J, Tamura K (2008) MEGA: a biologist-centric software for evolutionary analysis of DNA and protein sequences. Brief Bioinform 9:299–306

Librado P, Rozas J (2009) DnaSP v5: a software for comprehensive analysis of DNA polymorphism data. Bioinformatics 25:1451–1452

Ling B, Veazey RS, Luckay A, Penedo C, Xu K, Lifson JD, Marx PA (2002) SIVmac pathogenesis in rhesus macaques of Chinese and Indian origin compared with primary HIV infections in humans. AIDS 16:1489–1496

Lorenz E, Mira JP, Cornish KL, Arbour NC, Schwartz DA (2000) A novel polymorphism in the toll-like receptor 2 gene and its potential association with staphylococcal infection. Infect Immun 68:6398–6401

Matano T, Kobayashi M, Igarashi H, Takeda A, Nakamura H, Kano M, Sugimoto C, Mori K, Iida A, Hirata T, Hasegawa M, Yuasa T, Miyazawa M, Takahashi Y, Yasunami M, Kimura A, O'Connor DH, Watkins DI, Nagai Y (2004) Cytotoxic T lymphocyte-based control of simian immunodeficiency virus replication in a preclinical AIDS vaccine trial. J Exp Med 199:1709–1718

McMurray DN (2000) A nonhuman primate model for preclinical testing of new tuberculosis vaccines. Clin Infect Dis 30:S210–S212

Merx S, Neumaier M, Wagner H, Kirschning CJ, Ahmad-Nejad P (2007) Characterization and investigation of single nucleotide polymorphisms and a novel TLR2 mutation in the human TLR2 gene. Hum Mol Genet 16:1225–1232

Nakajima T, Ohtani H, Satta Y, Uno Y, Akari H, Ishida T, Kimura A (2008) Natural selection in the TLR-related genes in the course of primate evolution. Immunogenetics 60:727–735

Nei M, Gojobori T (1986) Simple methods for estimating the numbers of synonymous and nonsynonymous nucleotide substitutions. Mol Biol Evol 3:418–426

Ogus AC, Yoldas B, Ozdemir T, Uguz A, Olcen S, Keser I, Coskun M, Cilli A, Yegin O (2004) The Arg753Gln polymorphism of the human toll-like receptor 2 gene in tuberculosis disease. Eur Respir J 23:219–223

Osada N, Hashimoto K, Kameoka Y, Hirata M, Tanuma R, Uno Y, Inoue I, Hida M, Suzuki Y, Sugano S, Terao K, Kusuda J, Takahashi I (2008) Large-scale analysis of *Macaca fascicularis* transcripts and inference of genetic divergence between *M. fascicularis* and *M. mulatta*. BMC Genomics 9:90

Rhesus Macaque Genome Sequencing and Analysis Consortium (2007) Evolutionaly and biomedical insights from the rhesus macaque genome. Science 316:222–234

Saitou N, Nei M (1987) The neighbor-joining method: a new method for reconstructing Phylogenetic trees. Mol Biol Evol 4:406–425

Sanghavi SK, Shankarappa R, Reinhart TA (2004) Genetic analysis of Toll/Interleukin-1 receptor (TIR) domain sequences from rhesus macaque Toll-like receptors (TLRs) 1–10 reveals high homology to human TLR/TIR sequences. Immunogenetics 56:667–674

Schröder NW, Diterich I, Zinke A, Eckert J, Draing C, von Baehr V, Hassler D, Priem S, Hahn K, Michelsen KS, Hartung T, Burmester GR, Göbel UB, Hermann C, Schumann RR (2005) Heterozygous Arg753Gln polymorphism of human TLR-2 impairs immune activation by *Borrelia burgdorferi* and protects from late stage Lyme disease. J Immunol 175:2534–2540

Schwandner R, Dziarski R, Wesche H, Rothe M, Kirschning CJ (1999) Peptidoglycan- and lipoteichoic acid-induced cell activation is mediated by toll-like receptor 2. J Biol Chem 274:17406–17409

Shibata H, Yasunami M, Obuchi N, Takahashi M, Kobayashi Y, Numano F, Kimura A (2006) Direct determination of SNP haplotype of NFKBIL1 promoter polymorphism by DNA conformation analysis and its application to association study of chronic inflammatory diseases. Hum Immunol 67:363–373

Shinkai H, Tanaka M, Morozumi T, Eguchi-Ogawa T, Okumura N, Muneta Y, Awata T, Uenishi H (2006) Biased distribution of

single nucleotide polymorphisms (SNPs) in porcine Toll-like receptor 1 (TLR1), TLR2, TLR4, TLR5, and TLR6 genes. Immunogenetics 58:324–330

Singh KK, Schmidtke J (2005) Single nucleotide polymorphisms within the promoter region of the rhesus monkey tumor necrosis factor-alpha gene. Immunogenetics 57:289–292

Smith DG, McDonough JW, George DA (2007) Mitochondrial DNA variation within and among regional populations of longtail macaques (*Macaca fascicularis*) in relation to other species of the fascicularis group of macaques. Am J Primatol 69:182–198

Stevison LS, Kohn MH (2009) Divergence population genetic analysis of hybridization between rhesus and cynomolgus macaques. Mol Ecol 18:2457–2475

Tajima F (1989) Statistical method for testing the neutral mutation hypothesis by DNA polymorphism. Genetics 123:585–595

Takahashi-Tanaka Y, Yasunami M, Naruse T, Hinohara K, Matano T, Mori K, Miyazawa M, Honda M, Yasutomi Y, Nagai Y, Kimura A (2007) Reference strand-mediated conformation analysis (RSCA)-based typing of multiple alleles in the rhesus macaque MHC class I Mamu-A and Mamu-B loci. Electrophoresis 28:918–924

Texereau J, Chiche JD, Taylor W, Choukroun G, Comba B, Mira JP (2005) The importance of Toll-like receptor 2 polymorphisms in severe infections. Clin Infect Dis 41:S408–S415

Yang Z (2007) PAML 4: Phylogenetic analysis by maximum likelihood. Mol Biol Evol 24:1586–1591

Yim JJ, Adams AA, Kim JH, Holland SM (2006) Evolution of an intronic microsatellite polymorphism in Toll-like receptor 2 among primates. Immunogenetics 58:740–745

Zhang J, Rosenberg HF, Nei M (1998) Positive Darwinian selection after gene duplication in primate ribonuclease genes. Proc Natl Acad Sci U S A 95:3708–3713

OPEN ACCESS Freely available online

PLoS NEGLECTED TROPICAL DISEASES

Association of Mast Cell-Derived VEGF and Proteases in Dengue Shock Syndrome

Takahisa Furuta[1]*, Lyre Anni Murao[2], Nguyen Thi Phuong Lan[3], Nguyen Tien Huy[4], Vu Thi Que Huong[3], Tran Thi Thuy[5], Vo Dinh Tham[6], Cao Thi Phi Nga[6], Tran Thi Ngoc Ha[4], Yasukazu Ohmoto[7], Mihoko Kikuchi[4,8,9], Kouichi Morita[2,9], Michio Yasunami[4], Kenji Hirayama[4,9], Naohiro Watanabe[10]

1 Division of Infectious Genetics, Institute of Medical Science, University of Tokyo, Tokyo, Japan, **2** Department of Virology, Institute of Tropical Medicine (NEKKEN), Nagasaki University, Nagasaki, Japan, **3** Arbovirus Laboratory, Pasteur Institute, Ho Chi Minh City, Viet Nam, **4** Department of Immunogenetics, Institute of Tropical Medicine (NEKKEN), Nagasaki University, Nagasaki, Japan, **5** Children's Hospital No. 2, Ho Chi Minh City, Viet Nam, **6** Center for Preventive Medicine, Vinh Long, Viet Nam, **7** Free Radical Research Institute, Otsuka Pharmaceutical Co., Ltd., Tokushima, Japan, **8** Center of International Collaborative Research, Nagasaki University, Nagasaki, Japan, **9** Global COE Program, Nagasaki University, Nagasaki, Japan, **10** Department of Tropical Medicine, Jikei University School of Medicine, Tokyo, Japan

Abstract

Background: Recent *in-vitro* studies have suggested that mast cells are involved in Dengue virus infection. To clarify the role of mast cells in the development of clinical Dengue fever, we compared the plasma levels of several mast cell-derived mediators (vascular endothelial cell growth factor [VEGF], soluble VEGF receptors [sVEGFRs], tryptase, and chymase) and -related cytokines (IL-4, -9, and -17) between patients with differing severity of Dengue fever and healthy controls.

Methodology/Principal Findings: The study was performed at Children's Hospital No. 2, Ho Chi Minh City, and Vinh Long Province Hospital, Vietnam from 2002 to 2005. Study patients included 103 with Dengue fever (DF), Dengue hemorrhagic fever (DHF), and Dengue shock syndrome (DSS), as diagnosed by the World Health Organization criteria. There were 189 healthy subjects, and 19 febrile illness patients of the same Kinh ethnicity. The levels of mast cell-derived mediators and -related cytokines in plasma were measured by ELISA. VEGF and sVEGFR-1 levels were significantly increased in DHF and DSS compared with those of DF and controls, whereas sVEGFR-2 levels were significantly decreased in DHF and DSS. Significant increases in tryptase and chymase levels, which were accompanied by high IL-9 and -17 concentrations, were detected in DHF and DSS patients. By day 4 of admission, VEGF, sVEGFRs, and proteases levels had returned to similar levels as DF and controls. *In-vitro* VEGF production by mast cells was examined in KU812 and HMC-1 cells, and was found to be highest when the cells were inoculated with Dengue virus and human Dengue virus-immune serum in the presence of IL-9.

Conclusions: As mast cells are an important source of VEGF, tryptase, and chymase, our findings suggest that mast cell activation and mast cell-derived mediators participate in the development of DHF. The two proteases, particularly chymase, might serve as good predictive markers of Dengue disease severity.

Citation: Furuta T, Murao LA, Lan NTP, Huy NT, Huong VTQ, et al. (2012) Association of Mast Cell-Derived VEGF and Proteases in Dengue Shock Syndrome. PLoS Negl Trop Dis 6(2): e1505. doi:10.1371/journal.pntd.0001505

Editor: Maria G. Guzman, Tropical Medicine Institute Pedro Kourí (IPK), Cuba

Received May 9, 2011; **Accepted** December 20, 2011; **Published** February 21, 2012

Funding: This work was supported in part by grants-in-aid from the Japanese Ministry of Education, Culture, Sports, Science, and Technology (MEXT) for the 21c COE Program (2004–2008) and for Global COE Program (2008–2009), Nagasaki University, for funding the Overseas Laboratory for the Research Network for Infectious Diseases, and for the Tokutei Research, 2003–2005, and the Cooperative Research Grant of NEKKEN, 2010. The funders had no roles in study design, data collection and analysis, decision to publish, or preparation of the manuscript.

Competing Interests: The authors have declared that no competing interests exist.

* E-mail: furuta@ims.u-tokyo.ac.jp

Introduction

Dengue virus infection is associated with disease, ranging from Dengue fever (DF) to Dengue hemorrhagic fever (DHF) and/or Dengue shock syndrome (DSS). As severe diseases typically develop in individuals suffering secondary Dengue virus infection, host immunological factors appear to play a role in DHF and DSS [1]. DHF and DSS are characterized by increased vascular permeability and hemorrhagic manifestations [2], with the former phenotype recognized as the hallmark of these severe forms of Dengue. However, the cellular factors and immune molecules underling the development of DHF and DSS are not well understood.

Recent studies on Dengue virus infection have demonstrated that the serum levels of vascular endothelial cell growth factor (VEGF)-A (formerly VEGF) are elevated in DHF patients [3]. VEGF/vascular permeability factor (VPF) was first identified and characterized as a potent stimulator of endothelial permeability [4], and was shown to increase vascular permeability 50,000 fold more efficiently than histamine [5]. VEGF was subsequently reported to promote the proliferation, migration, and survival of endothelial cells [6]. VEGF is a member of a growing family of related proteins that includes VEGF-B, -C, -D, and placental growth factor [7]. A potential candidate for the VEGF-binding molecule is the soluble form of its receptor. At least two types of VEGF receptors are expressed on endothelial cells; both are

Author Summary

To clarify the involvement of mast cells in the development of severe Dengue diseases, plasma levels of mast cell-derived mediators, namely vascular endothelial cell growth factor (VEGF), tryptase, and chymase, were estimated in Dengue patients and control subjects in Vietnam. The levels of the mediators were significantly increased in Dengue hemorrhagic fever (DHF) and Dengue shock syndrome (DSS) patients compared with those of Dengue fever (DF) and control (febrile illness and healthy subjects) patients, and the soluble form of VEGF receptors (sVEGFR)-1 and -2 levels were significantly changed in the patients with severe disease. After 2–4 days of admission, the mediator levels had returned to similar levels as those of DF and control subjects. Furthermore, the levels of the Th17 cell-derived mast-cell activators IL-9 and -17 were increased in DHF and DSS. *In-vitro* production of VEGF in human mast cells was significantly enhanced in the presence of IL-9 when these cells were inoculated with Dengue virus in the presence of human Dengue virus-immune serum. As mast cells are an important source of VEGF, and tryptase and chymase are considered to be specific markers for mast cell activation, mast cells and mast cell-derived mediators might participate in the development of DHF/DSS.

transmembrane receptor tyrosine kinases, namely, VEGFR-1 or Fms-like tyrosine kinase 1 (Flt-1), and VEGFR-2 or kinase insert domain receptor (KDR) [8]. VEGFR-1 is expressed on monocyte-macrophage lineages other than endothelial cells, whereas VEGFR-2 is expressed primarily on endothelial cells and their progenitors [9,10]. In addition to its role in promoting endothelial permeability and proliferation, VEGF may contribute to inflammation and coagulation. For example, under *in-vitro* conditions, VEGF induces the expression of several types of cell adhesion molecules, including E-selectin, intercellular adhesion molecule 1 (ICAM-1), and vascular cell adhesion molecule 1 (VCAM-1), in endothelial cells and promotes the adhesion of leukocytes [11,12]. Moreover, VEGF signaling up-regulates tissue factor mRNA expression, and protein and procoagulant activities [13]. The proinflammatory/procoagulant effects of VEGF are mediated, at least in part, by the activation of the transcription factors NF-κB, Egr-1, and NFAT. VEGF has been implicated as a pathophysiological mediator in several human disease states, including rheumatoid arthritis, cancer, and inflammatory bowel disease [14–16].

Dengue patients typically exhibit increased levels of urinary histamine, which is a major granule product of mast cells and whose levels correlate with disease severity [17]. A large autopsy study of 100 DHF cases from Thailand found that mast cells in connective tissue around the thymus exhibited swelling, cytoplasmic vacuolation, and loss of granule integrity, which are suggestive of mast cell activation [18]. Although recent *in-vitro* studies have also reported the involvement of mast cells in Dengue virus infection [19,20], the potential role of mast cells in severe Dengue disease has not yet been explored.

The activation of mast cells, which reside mainly in tissues and are associated closely with blood vessels and nerves [21,22], is tightly linked with local increases in vascular permeability in allergic disease. Mast cells are key effector cells in IgE-dependent immune responses, such as those involved in the pathogenesis of allergic disorders or in certain instances of immunity to parasites [23]. Recent works have revealed another aspect of mast cell effector function, and mast cells play important roles in inflammation and host defenses against foreign pathogens [24,25].

Mast cells synthesize and release a range of biologically active substances, including proteases, biogenic amines, cytokines, chemokines, and lipid mediators [26]. Mast cell proteases are key protein components of secretory mast cell granules and are essential for innate antimicrobial inflammatory responses [27–29]. It is estimated that mast cell proteases account for >25% of total mast cell protein [30] and that human skin mast cells contain a total of ~16 μg tryptase and chymase per 10^6 cells [31]. Mast cell proteases, tryptase, and chymase are serine proteases with trypsin- or chymotrypsin-like substrate specificities, and are the major proteins stored and secreted by mast cells. Measurement of the serum (or plasma) levels of these proteases are recommended in the diagnostic evaluation of systemic anaphylaxis and mastocytosis, with total tryptase levels generally reflecting either the increased burden of mast cells in patients with all forms of systemic mastocytosis, or the decreased burden of mast cells associated with cytoreductive therapies in these disorders. Tryptase and chymase levels generally reflect the magnitude of mast cell activation and are typically elevated during systemic anaphylaxis. Secreted tryptase and chymase promote inflammation, matrix destruction, and tissue remodeling by several mechanisms, including the destruction of procoagulant, matrix, growth, and differentiation factors, and the activation of proteinase-activated receptors, urokinase, metalloproteinases, and angiotensin. In addition, these two serine proteases also modulate immune responses by hydrolyzing chemokines and cytokines, and can also suppress inflammation by inactivating allergens and neuropeptides responsible for inflammation and bronchoconstriction. Thus, similar to mast cells themselves, mast cell serine proteases play multiple roles in host defenses, which may be either beneficial or harmful depending on the specific conditions. As substantial levels of tryptase and chymase are only found in mast cells, these proteases are considered to be selective markers of mast cell activation [26]. The importance of cytokines and chemokines together with mast cells in the pathogenesis of Dengue virus infection has been demonstrated [19,20], however, the roles of the mast cell-specific proteases, tryptase and chymase, remain unclear.

Here, to determine the roles of mast cells and mast cell-derived mediators in DHF and DSS, we first measured the levels of VEGF, soluble forms of VEGFR-1 and -2, tryptase, and chymase in the plasma of Dengue patients and healthy control subjects. Moreover, because IL-9 has been reported as a T cell-derived growth factor of mast cells [32–34] and more recently has been implicated as a Th17-derived cytokine that contributes to inflammatory diseases, the involvement of IL-9 and IL-17 in Dengue infection was also investigated.

Methods

Study population and Dengue classification

The study was performed at two hospitals, Children's Hospital No. 2 in Ho Chi Minh City (HCMC) and the Center for Preventive Medicine in Vinh Long Province (VL), Vietnam. The enrolment was a consecutive sequence of hospitalized children at each hospital. The inclusion criteria on admission to the hospital were age (6 months to 15 years old) and ethnicity (Kinh race). A total of 103 subjects from HCMC and VL were enrolled in this study during 2002–2005 (Table 1). The patients were suspected to have Dengue virus infection based on clinical symptoms at admission. After hospitalization, the patients were diagnosed using standardized serology techniques, as described below, and the WHO (1997) classification criteria for Dengue virus infection [35]. It was reported that the sensitivity of WHO criteria for DSS in Vietnam was only 82%, mainly due to the lack of evidence for

Table 1. Characteristics of the Dengue patients.

Characteristic	DF (n = 19)	DHF (n = 43)	DSS (n = 41)
Sex (Male: Female)	12:7	22:21	21:20
Fever (mean±SD °C)	37.9±0.7	39.2±0.7	39.1±0.8
Primary infection	9	11	10
Secondary infection	10	32	31
Dengue Virus 1	1	16	4
Dengue Virus 2	1	14	6
Dengue Virus 3	2	4	0
Dengue Virus 4	0	0	0
Dengue Virus (-)	15	9	31
Conjunctive bleeding	0	0	1
Subcutaneous bleeding	0	39	40
GI bleeding*	0	0	5
Plasma leakage signs**	0	0	11
Hematocrit	0	43	41
Thrombocytopenia	0	43	41
Hepatomegaly	0	11	32
Narrow blood pressure	0	0	23
Neurologic disorder	0	0	1
Shock	0	0	41

Dengue classification was performed according to the definitions of the World Health Organization (WHO) [27]. DHF classification required fever or a history of acute fever, bleeding manifestation, and signs of plasma leakage, which included hemoconcentration, ascites, or pleural effusion with evidence of thrombocytopenia. DSS classification required DHF manifestation plus evidence of clinical hypovolemic shock. Cases of Dengue were confirmed by Dengue virus RNA detection by RT-PCR and IgM antibody capture (MAC) ELISA in the first or second paired samples. Dengue virus was isolated using plasma samples collected between days 4–6. Primary or secondary infection was determined by the AFRIMS method. Hct increase was determined by a >20% increase compared with the normal range of the population. Thrombocytopenia was defined as <100,000 platelets/mm^3.

*GI bleeding: Gastrointestinal bleeding.

**Plasma leakage signs: Ascites and pleural effusion.

doi:10.1371/journal.pntd.0001505.t001

thrombocytopenia [36]. Therefore, we basically followed the WHO criteria, but included patients lacking a significant reduction of platelet count, which accounted for no more than 11% of all DHF/DSS cases. Our classification scheme met the requirements of the simplified Integrated Management of Childhood Illness (IMCI) classification system, which is based on plasma leakage as a hallmark of severe dengue disease (DHF/DSS) [37].

Plasma samples were obtained from the 19 DF, 43 DHF, and 41 DSS patients on the day of admission, and an additional 189 plasma samples from healthy, unrelated school children living in HCMC and VL who had no symptoms of Dengue virus infection were collected as control samples. Eighteen (male: 12, female: 6) plasma samples were also collected from school children with a febrile illness (38.9±0.9°C: mean±SD) without an obvious source of infection, including Dengue virus.

This study was approved by the institutional ethical review committees of the Institute of Tropical Medicine, Nagasaki University, Jikei University School of Medicine in Tokyo, and the Pasteur Institute in Ho Chi Minh City. Written informed consent was obtained from the parents or legal guardians of the subjects upon enrollment.

Sample collection and serological diagnosis

The sample collection and serological diagnosis performed in this cohort study were identical to those reported in our previous study [38]. Blood samples were collected from patients with suspected Dengue infection at the time of admission (day 0) and twice during the following four days (days 2 and 4). Plasma samples were used for the titration of anti-Dengue virus IgM and IgG antibodies, virus isolation, and RT-PCR for the determination of viral serotype. Dengue virus infection was determined by previously established serologic criteria for IgM/IgG ELISAs to Dengue virus (DEN 1–4) and Japanese encephalitis virus in paired plasma, collected with at least three-day intervals [39]. IgM and IgG ELISAs were performed using kits obtained from the Pasteur Institute, HCMC and were considered positive if the ratio of optical density (OD) of test sera to the OD of negative control plasma was ≥2.3 [35]. The cases were diagnosed as secondary infection when the DV IgM-to-IgG ratio was <1.8 [40].

Dengue virus serotyping was performed as previously reported [38]. Briefly, acute plasma samples were used to inoculate C6/36 (*Aedes albopictus*) cells, virus was obtained, and the Dengue virus serotype was then identified using either a direct or indirect fluorescent antibody technique with monoclonal antibodies supplied by the Centers for Disease Control and Prevention (Fort Collins, CO, USA) [41]. Viral RNA was also extracted from the acute plasma samples with the QIAamp Viral RNA Mini Kit (Qiagen, Hilden, Germany) for the molecular detection of Dengue virus and confirmation of its serotype, as previously described [41]. Briefly, cDNA from the Dengue virus genome RNA was amplified with the Ready-to-go RT-PCR test kit (Amersham, MA, USA) using a consensus primer set (D1 and D2) [31]. The serotype was then determined by semi-nested PCR using specific primer sets (TS1, TS2, TS3, and TS4) to amplify serotype-specific fragments from the regions encoding the capsid and membrane proteins of Dengue virus [39].

ELISA assay

The plasma levels of VEGF (VEGF-A), sVEGFR-1, sVEGFR-2, IL-9, and IL-17 in samples from Dengue patient (DF, DHF, and DSS) and control groups (febrile illness and healthy subjects) were measured by ELISA kits (R&D Systems, Minneapolis, MN, or Peprotech Inc., Rocky Hill, NJ). The levels of tryptase or chymase in plasma from the Dengue patients and control groups, and the culture supernatants of mast cells were examined by ELISA kits (CSB, Newark, ED or Otsuka Pharmaceutical Co., Tokushima, Japan).

Dengue virus infection and in-vitro production of VEGF

The human mast cell/basophil line KU812 [42] and human mast cell line HMC-1 [43] were maintained in RPMI 1640 medium or IMDM (Invitrogen, Grand Island, NY). In the infection experiments, Dengue virus 2 (DV16681 strain) was propagated in the C6/36 cell line, and virus titers were then determined by plaque assay using BHK-21 cells [44]. In control experiments, the virus was rendered nonreplicative by placing a sample aliquot under a germicidal lamp (125 mJ/10 min, UV irradiation at 254 nm) at a distance of 5–6 cm, followed by a 30-min incubation on ice [44]. For infection, HMC-1 or KU812 cell pellets were adsorbed at 4°C for 90 min with aliquots of Dengue virus or UV-inactivated virus, Dengue virus in combination with human dengue virus immune serum (1:1,000 or 1:10,000 final dilution), UV-inactivated virus in combination with human dengue virus immune serum (1:1,000 or 1:10,000 final dilution), or Dengue virus in combination with normal human serum (1:1,000 final dilution) (premixed at 4°C for 90 min). Dengue virus

2 convalescent-phase sera were used in the antibody-dependent enhancement of Dengue virus infection. Mast cells were infected at a multiplicity of infection (MOI) of 3 plaque forming units (pfu)/cell. Following adsorption, cells were washed and plated in 96-well plates (0.25 mL/well) at 1×10^6 cells/mL and then incubated at 37°C in 5% CO_2 for 24 h. To examine the effects of IL-9 on the production of VEGF from mast cells, mast cells treated with Dengue virus and antibody were incubated with or without recombinant human IL-9 (200 ng/mL, Peprotech, Rocky Hill, NJ). Activation of mast cells with Compound (C) 48/80 (300 μg/ml, Sigma-Aldrich, St. Louis, MO) was used as a positive control, and the culture supernatant of C6/36 cells was used as a negative control. For the measurement of VEGF levels in culture supernatants, culture supernatants were collected from each well after incubation and then stored at −80°C until being subjected to ELISA.

Fluorescence microscopy

KU812 cells were inoculated with Dengue virus (MOI, 3) or Dengue virus-antiserum combinations. After incubation for 24 h, cells were fixed with 4% paraformaldehyde, washed, and then permeabilized with 0.1% saponin for 1 h at room temperature. Samples were then washed and incubated with mouse anti-Dengue virus monoclonal antibody 1B7 [45] and isotype-matched mouse IgG2a antibody (negative control, R&D Systems) on ice for 1 h, which were employed as primary antibodies. Subsequently, samples were washed and incubated with FITC-labeled anti-mouse IgG antibody (R&D Systems) for 1 h on ice. Cytospins were made for each sample, and positive cells were observed by fluorescence microscopy.

Statistical analysis

Plasma VEGF, sVEGFRs, IL-9, IL-17, tryptase, and chymase levels were compared between the Dengue (DF, DHF, or DSS) and control groups (febrile illness and healthy subjects) using the unpaired Student's t test. VEGF levels in the *in-vitro* experiments were also compared between the Dengue virus infection and control (UV-inactivated Dengue virus and Medium alone) samples using the unpaired Student's t test. A value of $p<0.05$ was considered statistically significant.

Results

VEGF and sVEGFR levels in Dengue patients

As mast cells are an important source of VEGF [46,47], we first measured VEGF levels in plasma samples from the DF (n = 19), DHF (n = 43), and DSS (n = 41) patient groups, and the control group, which consisted of febrile illness and healthy subjects. On day 0 (admission), the VEGF plasma levels were significantly higher in DHF and DSS than those in DF, and febrile illness and healthy subjects (Fig. 1A). The sVEGFR-1 levels in plasma were higher in DSS than those in DF, DHF, febrile illness and healthy subjects (Fig. 1B). In contrast with sVEGR-1, the levels of sVEGFR-2 were dramatically decreased in DHF and DSS compared with DF or febrile illness and healthy subjects (Fig. 1C).

We next examined the levels of VEGF and sVEGFRs in DHF (n = 21) and DSS (n = 27) patients during the admission period (Fig. 2). The VEGF levels in DHF and DSS, and sVEGFR-1 levels in DSS were significantly higher than those of DF or healthy controls on the day of admission (day 0); however, 2–4 days later (convalescence), their levels had gradually declined to comparable levels with DF, febrile illness, and healthy subjects by the convalescent phase (day 4; VEGF DF: 0.61±+0.24 ng/ml, febrile illness: 0.57±0.11 ng/ml, and healthy subjects: 0.52±0.17 ng/ml; sVEGFR-1 DF: 180.9+55.3 pg/ml, DHF: 223.6±136 pg/ml, febrile illness: 201.3±167.1 pg/ml, and healthy subjects: 195.1±59.1 pg/ml). The plasma levels of sVEGFR-2 in DHF and DSS patients were significantly lower compared to those of DF, febrile illness, and healthy subjects; however, the levels were comparable between these groups by day 4 (Fig. 2). Taken together, these findings suggested the possibility that VEGF and sVEGFRs participated in severe Dengue virus infection.

Tryptase and chymase levels in Dengue patients

We also measured the tryptase and chymase levels in plasma collected from the Dengue patients (day 0) and controls by ELISA. Plasma tryptase levels increased significantly in DHF and DSS compared with DF, febrile illness, and healthy subjects (Fig. 3). In contrast, the chymase levels were increased significantly in DSS compared with DF, DHF, febrile illness, and healthy subjects (Fig. 3). We next measured the plasma levels of tryptase and chymase in DHF (n = 21) and DSS (n = 27) patients during the admission period and found that the protease levels had gradually declined by days 2 and 4 to a comparable level with those of DF, febrile illness, and healthy subjects (chymase DF: 4.8±2 ng/ml, DHF: 6.7±2.4 ng/ml, febrile illness: 6.2±2 ng/ml, healthy subjects: 4.5±1.3 ng/ml, tryptase DF: 7.4±4.3 ng/ml, febrile illness: 6.7±2.6 ng/ml, healthy subjects: 7.7±3.4 ng/ml) (Fig. 2). These results suggested that mast cells and mast cell-derived proteases participated in the severe form of Dengue virus infection.

IL-4, IL-9, and IL-17 levels in Dengue patients

As IL-9 has been reported as a T cell-derived mast cell growth factor [32–34] and more recently, is implicated as a Th17-derived cytokine that can contribute to inflammatory diseases, we investigated the involvement of IL-9 and IL-17 in Dengue virus infection. The levels of IL-9 and IL-17 in Dengue patients on day 0, and those in blood samples collected from febrile illness and healthy subjects were measured by ELISA. The analysis showed that IL-9 and IL-17 levels were significantly increased in DHF and DSS compared with those in DF, febrile illness, and healthy subjects (Figs. 4A and B).

Although these results suggested that IL-9 and IL-17 participate in Dengue virus infection, IL-9 may act additively or synergistically with other factors, such as other Th2 cytokines, to induce optimal mast cell responses. To examine the possibility that Th2 cytokines affect mast cell responses in Dengue virus infection, IL-4 levels were also examined in plasma from Dengue patients and control groups (Fig. 4C). We found comparable levels of IL-4 between Dengue patients and control groups, suggesting the involvement of IL-9 and -17 in Dengue virus infection.

In-vitro production of VEGF in mast cells

To investigate if Dengue virus induces VEGF production from mast cells, the *in-vitro* production of VEGF in the human mast cell lines KU812 and HMC-1 was examined. KU812 and HMC-1 cells were inoculated with Dengue virus in the presence of either human Dengue virus-immune or normal human serum, and VEGF levels in the culture medium were assessed 24 h after viral inoculation. As the antibody-dependent enhancement of infection in KU812 and HMC-1 cells was observed at 1:1,000 and 1:10,000 dilutions of human Dengue virus-immune serum in preliminary experiments (data not shown), a 1:1,000 dilution was used in the *in-vitro* experiments in this study.

The production of VEGF was observed in both KU812 and HMC-1 cells after exposure to Dengue virus in the presence human Dengue virus-immune serum, however, VEGF levels were higher in KU812 cells (Table 2). No significant increase of VEGF